

## Supporting Information for

### In situ measurement of CuO and Cu(OH)<sub>2</sub> nanoparticle dissolution rates in quiescent freshwater mesocosms

Brian E. Vencalek<sup>†</sup>, Stephanie N. Laughton<sup>†</sup>, Eleanor Spielman-Sun<sup>†</sup>, Sonia M. Rodrigues<sup>‡</sup>, Jason M. Unrine<sup>§, #</sup>, Gregory V. Lowry<sup>†, \*</sup>, Kelvin B. Gregory<sup>†</sup>.

<sup>†</sup>Department of Civil and Environmental Engineering, Carnegie Mellon University, Pittsburgh, Pennsylvania 15213, United States

<sup>‡</sup>Centre for Environmental and Marine Studies (CESAM), Department of Chemistry, Universidade de Aveiro, 3810-193 Aveiro, Portugal

<sup>§</sup>Center for Environmental Implications of NanoTechnology (CEINT), Duke University, Durham, North Carolina 27708-0287, United States

<sup>#</sup>Department of Plant and Soil Sciences, University of Kentucky, Agricultural Science Center, Lexington, KY 40546, United States

\*Address correspondence to glowry@cmu.edu

#### Table of Contents

<b>Table S1. CBNP Dissolution Rates from Selected Studies</b>	<b>S2</b>
<b>Additional Materials and Methods Detail</b>	<b>S3</b>
<b>Visual MINTEQ 3.0 Chemical Equilibrium Models</b>	<b>S6</b>
<b>Particle characterization</b>	<b>S10</b>
<b>First-order Dissolution Rtes Constants and 95% CI</b>	<b>S10</b>
<b>Photos of Dialysis Experimental setup</b>	<b>S16</b>
<b>Mesocosm temperature and pH data</b>	<b>S17</b>
<b>References</b>	<b>S18</b>

**Table S1. CBNP Dissolution Rates from Selected Studies.**

<i>nanoparticle</i>	<i>concentration</i> ( $\text{mg L}^{-1}$ )	<i>media</i>	<i>first-order dissolution</i> <i>rate coefficient</i> ( $\text{hr}^{-1}$ )	<i>t</i> (h)	<i>% dissolved</i> <i>at t</i>	<i>reference</i>
CuNP	20	50 mM acetate, pH = 4.9	-	30	60	Wang et al. <sup>1</sup>
CuNP	10	0.5 mM PBS, pH=7	-	24	< 4	Adeleye et al. <sup>2</sup>
CuNP	10	Simulated groundwater, pH=7.5	-	48	< 10	Conway et al. <sup>3</sup>
CuNP	100	5 ppm BSA, 100 mM PBS, pH = 7.0	1.36	24	1	Wang et al. <sup>4</sup>
CuONP	10	0.5 mM PBS, pH=7	-	24	<1	Adeleye et al. <sup>2</sup>
CuONP	10	Simulated groundwater, pH=7.5	-	48	< 1	Conway et al. <sup>3</sup>
CuONP	80	10 mM NaNO <sub>3</sub> , pH=7.0	-		0.025	Ma et al. <sup>5</sup>
CuONP – spherical	750	1 mM NaNO <sub>3</sub> , pH=6.7	0.49	180	0.17	Misra et al. <sup>6</sup>
CuONP – rod shaped	750	1 mM NaNO <sub>3</sub> , pH=6.7	0.05	180	0.05	Misra et al. <sup>6</sup>
CuONP	1	Reconstituted water w/100 mM MOPS, pH=7.5	-	48	0.19	Son et al. <sup>7</sup>

## ADDITIONAL MATERIALS AND METHODS DETAIL

**Water Characterization.** Water samples from three freshwater emergent wetland mesocosms were collected at the Duke Forest in Durham, NC, pooled, and stored at 4°C prior to use. The construction and preparation of the mesocosm boxes has been described elsewhere<sup>8</sup>. Briefly, mesocosm water is a groundwater aged in loam soils in the presence of several species of common wetland vegetation. The water is soft and mildly alkaline, with a low concentration of TDS and a pH of 7.7. DI water had a slightly acidic pH (~5.8). Before use in the dissolution studies, the mesocosm water was aerated for thirty (30) minutes to prevent reducing conditions, centrifuged at 6,000 g for ten minutes to remove large particles and plant matter, and the supernatant was filter-sterilized with a 0.22 µm PVDF membrane vacuum filtration unit (SoCal Biomedical; Newport Beach, CA) to remove colloidal and suspended solids. The latter steps were performed to prevent biological fouling of the dialysis membrane and to isolate effects of solution chemistry on dissolution. Samples of mesocosm water were analyzed according to standard methods. A full description of the methods and equipment is provided in the SI. Cu speciation was estimated with the thermodynamic modeling software Visual MINTEQ 3.0<sup>9</sup> using the mesocosm water quality data presented in Table S2. A detailed explanation of the modeling assumptions and input parameters is provided in the SI.

**Nanoparticle Characterization.** Two CBNPs were investigated in this study: copper oxide nanoparticles (CuONP) and a commercially available fungicide reported to be primarily spertinite (Cu(OH)<sub>2</sub>).<sup>10</sup> Spherical CuONP aggregates with a nominal average primary particle size of 40nm were purchased from U.S. Research Nanomaterials (Houston, TX). Complete characterization of the particles can be found in Ma et al.<sup>5</sup> The commercial CBNP mixture was purchased as Kocide 3000<sup>®</sup> (Certis, USA, Columbia MD). All materials were used as received. The ζ-potential and hydrodynamic diameter (HDD) of the Kocide 3000<sup>®</sup> and CuO particles were measured using a Malvern Zetasizer Nano ZS in a 0.1 mM KNO<sub>3</sub> solution (pH 5.8) and filtered mesocosm water (pH 7.7). The phase of Kocide 3000<sup>®</sup> was

determined by powder X-ray diffraction (XRD), and the particle morphology was assessed using a Jeol 2010F high resolution field-emission gun transmission electron micrograph (HR-TEM; Tokyo, Japan).

**Dissolution Experiments.** All dissolution experiments were carried out in filtered mesocosm water or DI water using slight modification of previously described techniques.<sup>11</sup> Float-A-Lyzer G2 membrane dialysis devices (Spectrum Labs; Rancho Dominguez, CA) with a molecular weight cutoff of 8–10 kDa and a working volume of five milliliters were used to separate Cu nanoparticles from the dissolved Cu species. For CuONP experiments, a 100 mg L<sup>-1</sup> stock suspension was prepared and dispersed in ultrapure DI water. The stock was diluted to 1 mg L<sup>-1</sup> (CuO) with either ultrapure DI water or filtered mesocosm water. For Kocide 3000®, a 20 mg L<sup>-1</sup> stock solution (Cu(OH)<sub>2</sub>) was prepared in ultrapure DI water, dispersed, and diluted to 1 mg L<sup>-1</sup> with either ultrapure DI water or mesocosm water. For the Cu(NO<sub>3</sub>)<sub>2</sub> control experiments, a 6.4 mg L<sup>-1</sup> stock solution was prepared in ultrapure DI water. The stock was diluted to 1 mg L<sup>-1</sup> with ultrapure DI and 0.4 mg L<sup>-1</sup> with mesocosm water. The dispersion protocol was identical for CuONP and Kocide 3000® and consisted of sequentially sonicating on ice for ten minutes in a Branson model 5200 ultrasonic cleaner followed by probe sonicating with a Fisher Scientific 550 Sonic Dismembrator on ice at ten second intervals for a total of sixty seconds. The dialysate consisted of five milliliters of the diluted CuONP, Kocide 3000®, or Cu(NO<sub>3</sub>)<sub>2</sub> stock solutions (1 mg L<sup>-1</sup> total CuNP or Cu(NO<sub>3</sub>)<sub>2</sub>) and the dialysis solvent consisted of 20 mL of either ultrapure DI water or filtered mesocosm water. The experimental dialysis tubes were placed in 50 mL centrifuge tubes containing the dialysis solvent, laid horizontally on an orbital shaker, and mixed at 200 rpm at 20 °C ± 2 °C. Each experiment was performed in duplicate. The media in the dialysate reservoir was replaced with fresh media after every sample was collected to maintain the maximum concentration gradient between the dialysis membrane and the bulk solution. Samples were acidified to 2% HNO<sub>3</sub> using 70% HNO<sub>3</sub> for total Cu analysis by inductively coupled plasma – mass spectrometry (ICP-MS) using an Agilent Technologies 7700 (Santa Clara, CA, USA). The baseline copper concentration of the mesocosm water was determined by preparing two (2) extra centrifuge tubes with fresh media for each experimental condition and acidifying and analyzing with the same methods as the experimental samples. The baseline copper

concentration, which varied from 7 - 25  $\mu\text{g L}^{-1}$ , was then subtracted from the copper concentration measured in the mesocosm water experimental samples to determine the copper recovered due to dissolution and diffusion through the dialysis membrane. The pH of the DI and mesocosm water for the  $\text{Cu}(\text{NO}_3)_2$ , Kocide 3000<sup>®</sup>, and CuONP samples was measured after sample collection but prior to acidification and was found to be  $5.8 \pm 0.3$  and  $7.7 \pm 0.3$ , respectively.

**Stagnant Dissolution Experiments.** Dissolution was also determined under more environmentally relevant ‘no-mix’ conditions. One experiment was performed in a large tank of DI water to avoid buildup of Cu concentration in the dialysate (Figure S10). A second was performed *in-situ* at the Duke mesocosm facility (Figures S11 and S12). Dialysis tube preparation was identical to the previously described protocol except that all tubes were secured within flotation devices and placed upright at the start of the experiment. Environmental conditions in the mesocosms fluctuated during the course of the experiments, with the pH fluctuating between 6.7 and 9.1 and the water temperature varying between 10 and 16 °C (Figure S14) over 72 hours. To determine the rate of Cu dissolution, a dialysis tube (Figure S13) was sacrificially sampled at specified time points over 72 hours. Five milliliters of aqueous suspension was aspirated from the tube and acidified in 2%  $\text{HNO}_3$  for subsequent Cu analysis by ICP-MS. In addition, the dialysis membranes were digested to determine the attached Cu remaining after a given experimental duration. Membranes were digested in 10 milliliters of 35%  $\text{HNO}_3$  for two hours at 105 °C and diluted to 5%  $\text{HNO}_3$  for Cu analysis by ICP-MS. It was assumed that all Cu remaining in the tube existed as a particle and that the difference between the initial mass of Cu and the mass of Cu in the tube at the sampling interval represented the dissolved mass.

**Mesocosm Water Characterization.** Conductivity and pH were measured using an Accumet™ XL benchtop meter (Fisher Scientific™) with pH and conductivity probes and alkalinity was measured using a titration kit (Hach). Total organic carbon (TOC) was analyzed using an InnovOx Laboratory TOC Analyzer (GE Analytical Instruments) and anions were analyzed using a Dionex ICS-5000 (Thermo

Scientific) with a Dionex IonPac™ AS11-HC column. Samples were acidified in 2% HNO<sub>3</sub> and were analyzed for metals by Inductively Coupled Plasma – Mass Spectrometry (ICP-MS) using an Agilent Technologies 7700 Series ICP-MS. The water quality data is presented in Table S2.

### Visual MINTEQ 3.0 Chemical Equilibrium Models

*Equilibrium Copper Speciation as a Function of pH and DOC.* Equilibrium dissolved Cu concentrations were estimated for a simple system using Visual MINTEQ 3.0<sup>9</sup>. Total copper was input as 1 mg L<sup>-1</sup> Cu<sup>2+</sup> and the temperature was set to 25 °C. The concentration of DOC was varied from 0, 1, and 10 mg L<sup>-1</sup> and the pH was varied from 5 to 9 for each DOC condition. Ionic strength was calculated from the components. The results are presented in Figures S1.

**Table S2. Mesocosm Water Characterization<sup>a</sup>**

<i>parameter</i>	<i>unit</i>	<i>average</i>		<i>standard deviation</i>
pH	-	7.8	±	0.05
Specific Conductance	µS/cm	90.1	±	0.12
TDS (calculated)	mg L <sup>-1</sup>	60.4	±	0.08
Alkalinity	mg L <sup>-1</sup> as CaCO <sub>3</sub>	23	±	2
Hardness (calculated)	mg L <sup>-1</sup> as CaCO <sub>3</sub>	32	-	-
Anions				
Chloride	mg L <sup>-1</sup>	5.4	±	0.02
Sulfate	mg L <sup>-1</sup>	4.2	±	0.02
Nitrate	mg L <sup>-1</sup>	0.8	±	0.20
Nitrite	mg L <sup>-1</sup>	0.34	±	0.001
TC (diss.)	mg L <sup>-1</sup>	12.3	±	0.4
TOC (diss.)	mg L <sup>-1</sup>	8.8	±	0.4
IC (diss.)	mg L <sup>-1</sup>	3.5	±	0.1
Cations				
Na	mg L <sup>-1</sup>	6.5	±	0.12
Mg	mg L <sup>-1</sup>	2.9	±	0.045
Ca	mg L <sup>-1</sup>	8.0	±	0.19
K	mg L <sup>-1</sup>	0.60	±	0.01
Al	µg L <sup>-1</sup>	17.2	±	0.9

Cations (continued)				
<i>parameter</i>	<i>unit</i>	<i>average</i>		<i>standard deviation</i>
Fe	$\mu\text{g L}^{-1}$	68.8	$\pm$	11.9
Se	$\mu\text{g L}^{-1}$	3.3	$\pm$	1.7
Sr	$\mu\text{g L}^{-1}$	47.3	$\pm$	0.8
Ba	$\mu\text{g L}^{-1}$	17.3	$\pm$	0.6

<sup>a</sup>All analyses performed in triplicate

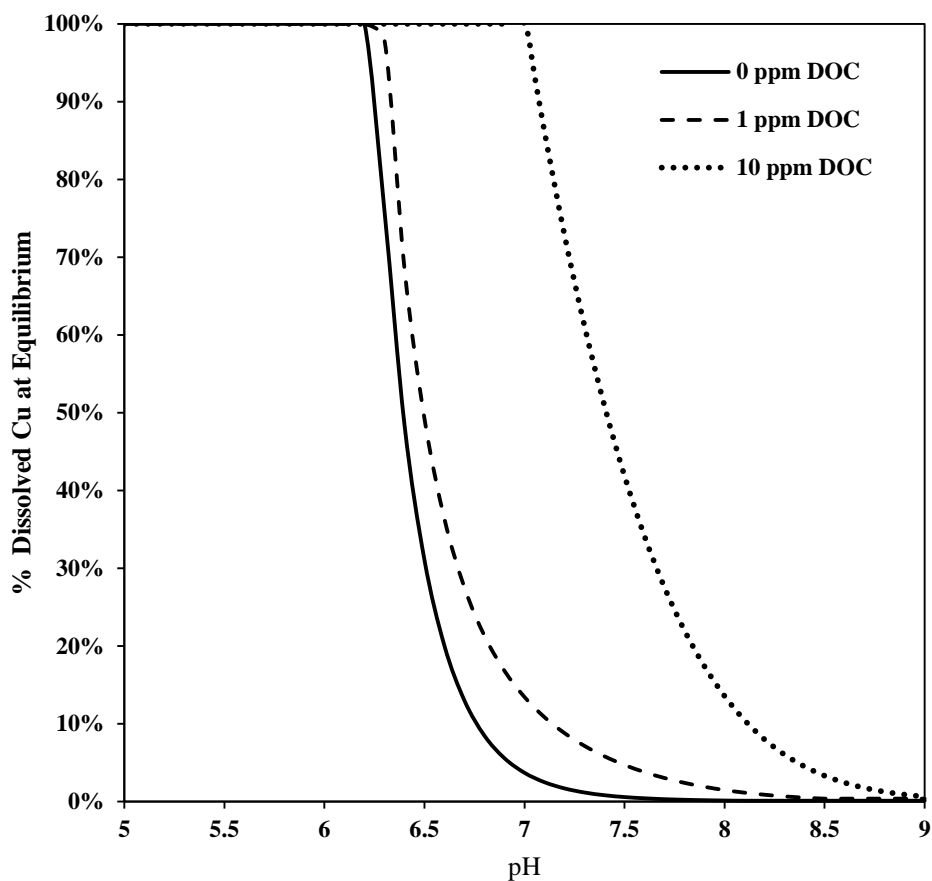


**Figure S1. Change in dissolved copper as a fraction of total copper for different DOC concentrations (0,1, and 10 mg L<sup>-1</sup>) and pH values (T = 25 °C).**

Figures S1 illustrates the effect of DOC and pH on the dissolved fraction of Cu at equilibrium, suggesting that these two factors may influence the rate of CBNP dissolution.

*Mesocosm Water Model Input Parameters.* Equilibrium copper speciation was predicted in mesocosm water using Visual MINTEQ 3.0<sup>9</sup>. The model parameters and input components for the mesocosm water system were adapted from Table S2 and are listed in Table S3.

**Table S3. Visual MINTEQ 3.0 Chemical Equilibrium Model Input Parameters and System**

**Components.**

<i>parameter</i>	<i>value</i>
pH	7.8
Ionic Strength	0.00035
Temperature °C	20
pe	0

<i>component</i>	<i>concentration (mg L<sup>-1</sup>)</i>
CO <sub>3</sub> <sup>-2</sup>	3.5
Cl <sup>-</sup>	5.4
S (SO <sub>4</sub> <sup>2-</sup> )	4.2
NO <sub>3</sub> <sup>-1</sup>	0.8
NO <sub>2</sub> <sup>-1</sup>	0.34
DOC (Gaussian DOM)	8.8
DOM1	0
Cu <sup>+2</sup>	0.8
Na <sup>+1</sup>	6.5
Mg <sup>+2</sup>	2.9
Ca <sup>+2</sup>	8
K <sup>+1</sup>	0.60
Fe <sup>+3</sup>	0.07
Al <sup>+3</sup>	0.02
Ba <sup>+2</sup>	0.02
Sr <sup>+2</sup>	0.05

*Model Output.* Visual MINTEQ modeling indicated that at concentrations of  $800 \mu\text{g L}^{-1}$  and  $400 \mu\text{g L}^{-1}$ , which is roughly equivalent to 1 ppm CuONP and 2 ppm Kocide 3000<sup>®</sup> respectively, Cu in DI water at equilibrium is primarily dissolved free  $\text{Cu}^{2+}$  ion. All other species ( $\text{Cu}_x(\text{OH})_y^{2x-y}$ ) comprised less than 2% of total dissolved Cu. In contrast, only  $25 \mu\text{g L}^{-1}$  of total Cu is as freely dissolved  $\text{Cu}^{2+}$  at equilibrium in mesocosm water, with the remainder precipitating as tenorite (CuO) and cupric ferrite. The predominant dissolved copper species in mesocosm water are Cu-DOC (75%) complexes followed by  $\text{CuOH}^+$  (11%), free  $\text{Cu}^{2+}$  ion (8%), and  $\text{CuCO}_3$  (6%). The results of the equilibrium speciation model are presented in Figure S2.

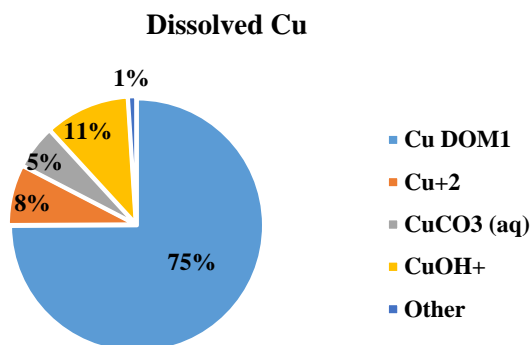


**Figure S2. Visual MINTEQ 3.0 Chemical Equilibrium Model Output for Cu in Mesocosm Water.**

## Particle Size and $\zeta$ potential

Samples of mesocosm water were filtered with a 3kDa filter to remove colloids. Samples were prepared at 1 ppm CBNP and re-run at 10 ppm due to low count rates.

**Table S4. Primary Peak Intensity-Averaged Hydrodynamic Diameter (IAHDD) and  $\zeta$  Potential in DI with 0.1mM NaNO<sub>3</sub> (pH=5.8) and Mesocosm water (pH=7.8).**

	<i>concentration (ppm)</i>	<i>medium</i>	<i>IAHDD (nm)</i>	<i>PDI</i>	<i><math>\zeta</math> potential (mV)</i>	<i>Std Dev. (mV)</i>
Kocide 3000®	1	a	427	0.551	-	-
CuONP	1	a	281	0.58	-	-
Kocide 3000®	1	b	374	0.674	-	-
CuONP	1	b	338	0.781	-	-
Kocide 3000®	10	a	299	0.49	-40	5.5
CuONP	10	a	342	0.597	-29.8	4.74
Kocide 3000®	10	b	396	0.453	-30.5	8.8
CuONP	10	b	392	0.342	-26.6	6.3

<sup>a</sup>0.1 mM NaNO<sub>3</sub> (pH=5.8)

<sup>b</sup>Mesocosm water (pH=7.8)

**Table S5. First-order Dissolution Rate Constants**

<i>CBNP</i>	<i>water</i>	<i>Mixing Condition</i>	<i>k<sub>diss</sub> (hr<sup>-1</sup>)</i>	<i>95% LCL<sup>a</sup></i>	<i>95% UCL<sup>b</sup></i>	<i>dissolution half-life (hr)</i>
Kocide 3000®	DI	well-mixed	0.056	0.019	0.094	0.87
	Mesocosm	well-mixed	0.0058	0.0041	0.0076	8.4
	DI	stagnant	0.0078	0.0061	0.0095	6.3
	Mesocosm	stagnant	0.0015	0.0011	0.0019	33
CuONP	DI	well-mixed	0.0017	0.0014	0.0019	30
	Mesocosm	well-mixed	0.00067	0.00056	0.00078	73
	DI	stagnant	0.0015	0.0011	0.0020	32
	Mesocosm	stagnant	0.0017	0.0012	0.0022	29

<sup>a</sup>LCL = Lower Confidence Limit

<sup>b</sup>UCL = Upper Confidence Limit

### X-Ray Diffraction Data for Kocide 3000® and CuONP

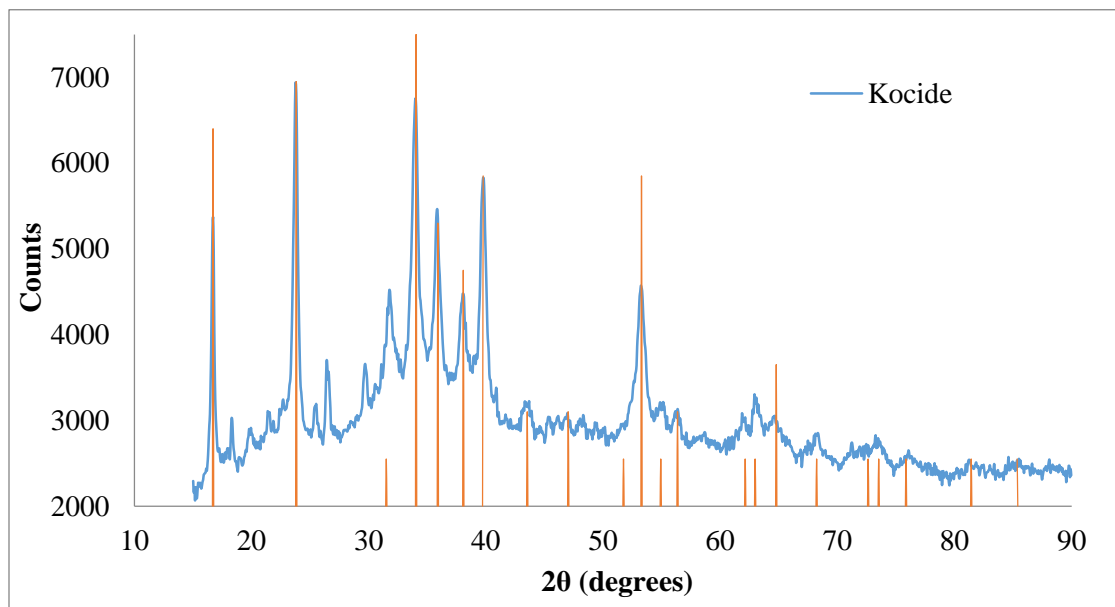


**Figure S3. XRD pattern of Kocide 3000®. The pattern matches well with the pattern of  $\text{Cu}(\text{OH})_2$  (Reference code :00-035-0505), indicating that the main crystalline component of Kocide is  $\text{Cu}(\text{OH})_2$ . Some smaller peaks are indicative of other minor Cu phases.**

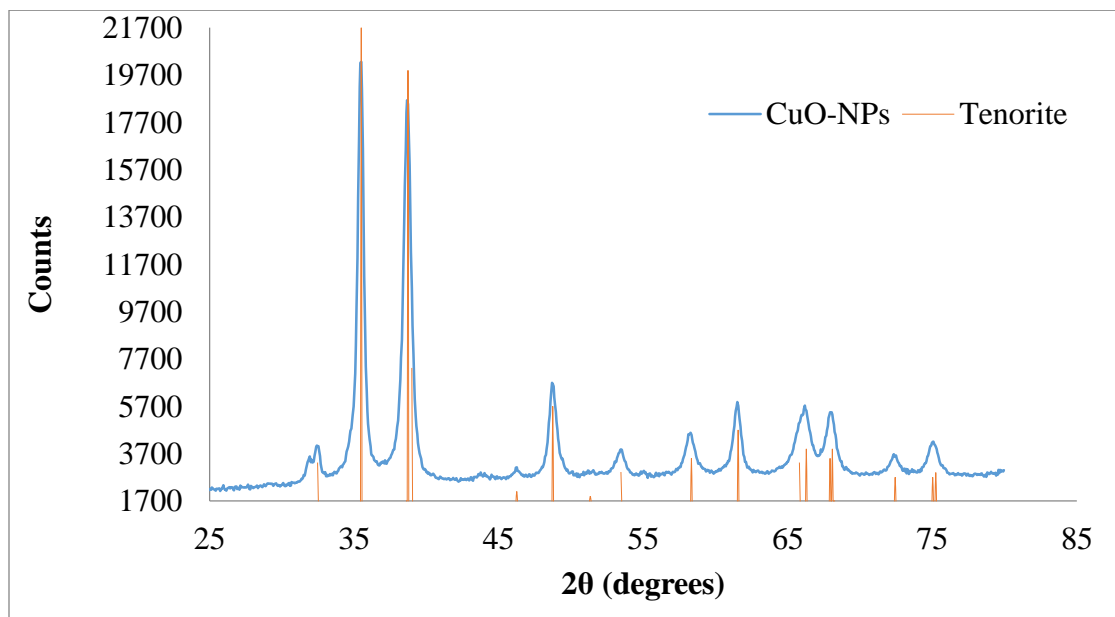


**Figure S4. XRD pattern of CuO-NPs. The pattern matches well with the pattern of the mineral phase Tenorite (Reference code : 00-045-0937), indicating the main crystalline components of CuO-NPs are Tenorite as previously reported<sup>5</sup>.**

**Kocide 3000<sup>®</sup> TEM and EDS.**

Gold grids were used to image particles. Both micron and nano-scale  $\text{Cu}(\text{OH})_2$  particles were visible (Figure S5). Samples were run on EDS was to determine the elemental composition (Figure S6)

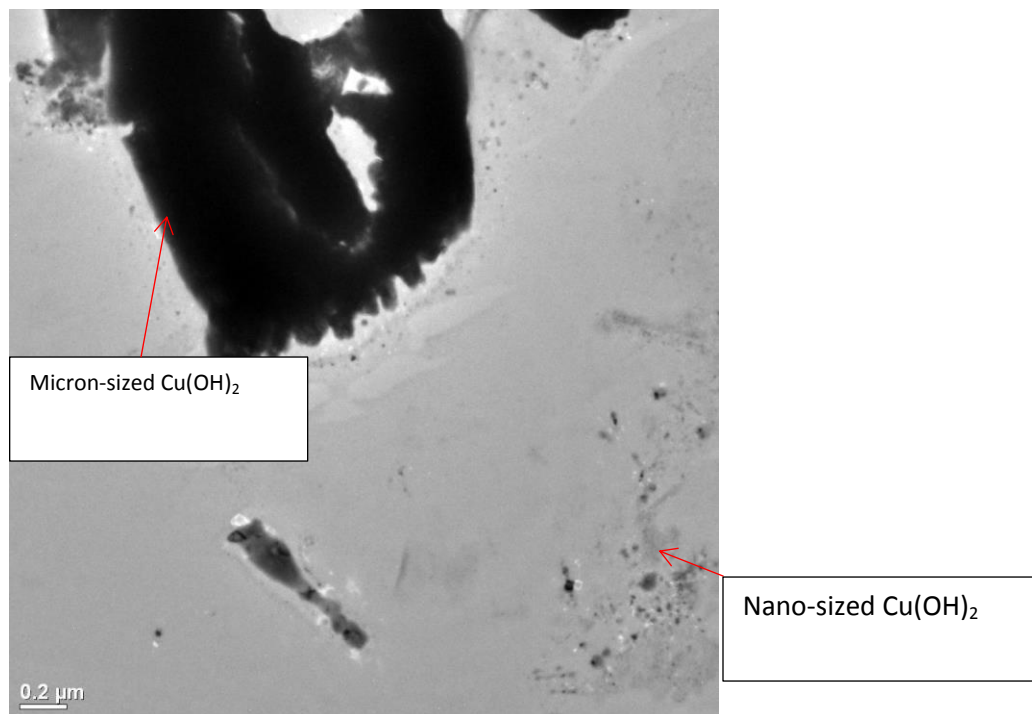


**Figure S5. TEM image of micron and nano-scale  $\text{Cu}(\text{OH})_2$  particles in Kocide 3000<sup>®</sup>.**

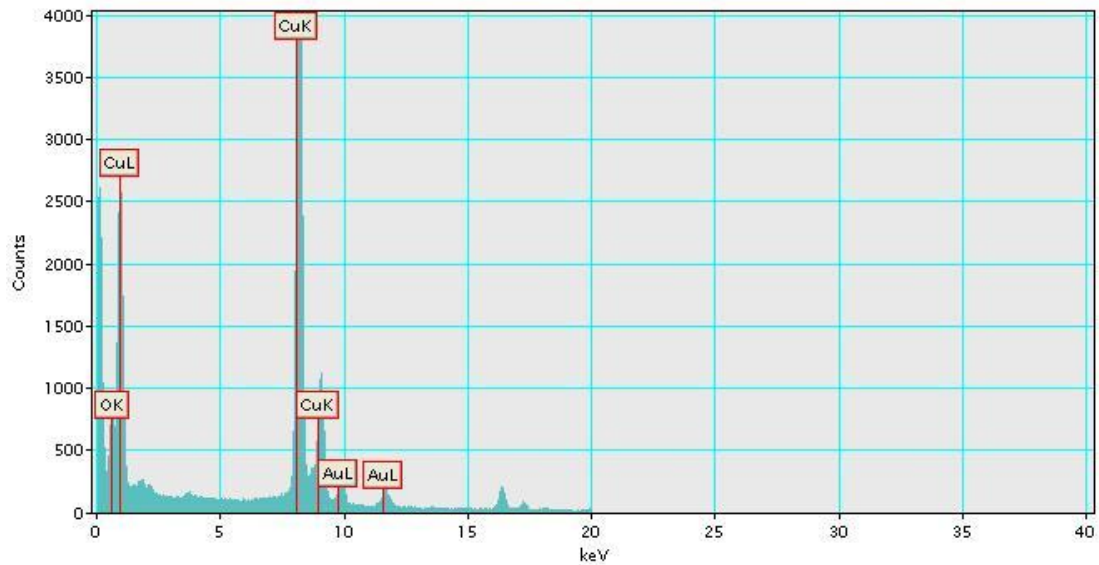


**Figure S6. EDS image of micron and nano-scale  $\text{Cu}(\text{OH})_2$  particles in Kocide 3000<sup>®</sup>.**

$\text{Cu}(\text{OH})_2$  particles in the nano-size range were identified (Figure S7), but the results indicated that the NPs were not stable under the TEM beam. Particles resembled rods at low magnification (around 40 K). After taking an image at higher magnification for the same spot, particles appeared spherical. It is possible that the spherical-shaped NPs are an artifact generated by TEM strong beam (200 kV).

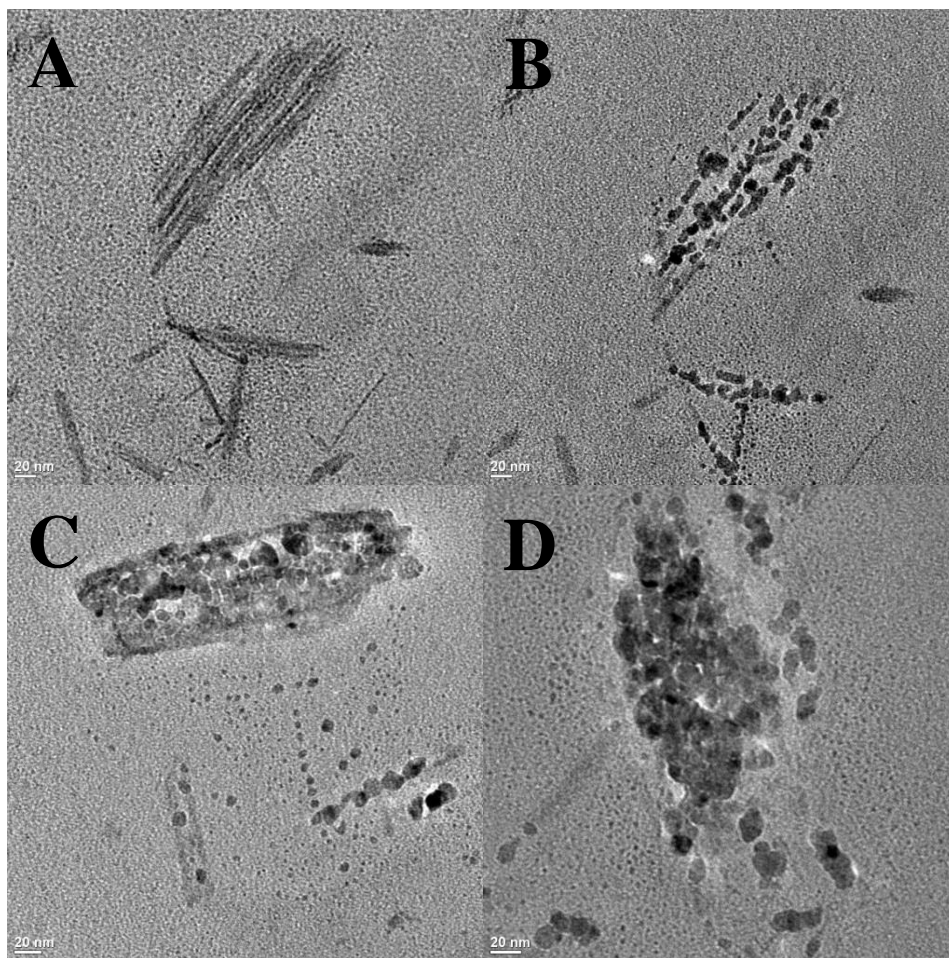


**Figure S7. TEM image of micron and nano-scale  $\text{Cu}(\text{OH})_2$  particles in Kocide 3000<sup>®</sup>. A) Before high resolution image B) After high resolution image C and D) two(2) images of  $\text{Cu}(\text{OH})_2$  NPs after running EDS on these spots.**

Figures S8 and S9 depict what appear to be polymer due to the strong carbon signal on the EDS spectrum. Si and other elements peaks were present on the EDS spectrum as well. The average diameter of spherical particles is 6 nm and the average length of rods is 120 nm.

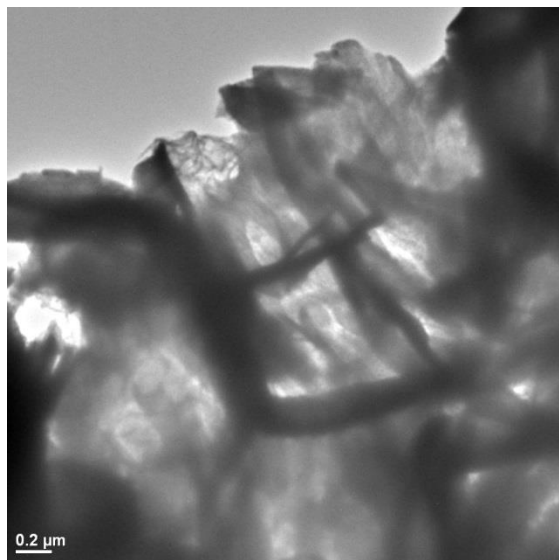


**Figure S8. TEM image of Kocide 3000®.**

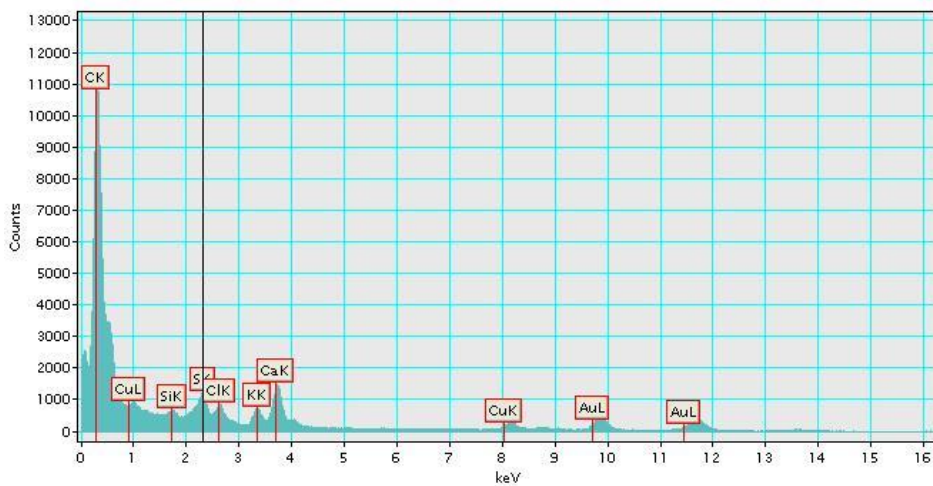


**Figure S9. EDS image of Kocide 3000®.**

**Figure S10. ‘No mixing’ CBNP dissolution in DI water reservoir (3.5 L).**



**Figure S11. Mesocosm facility at Duke Forest in Durham, NC.**



**Figure S12. *In-situ* CBNP dissolution experiment at mesocosm facility.**



Figure S13. Dialysis device.

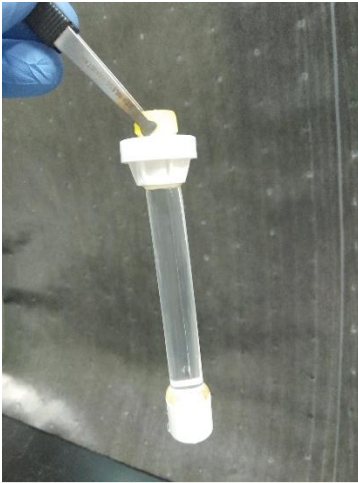
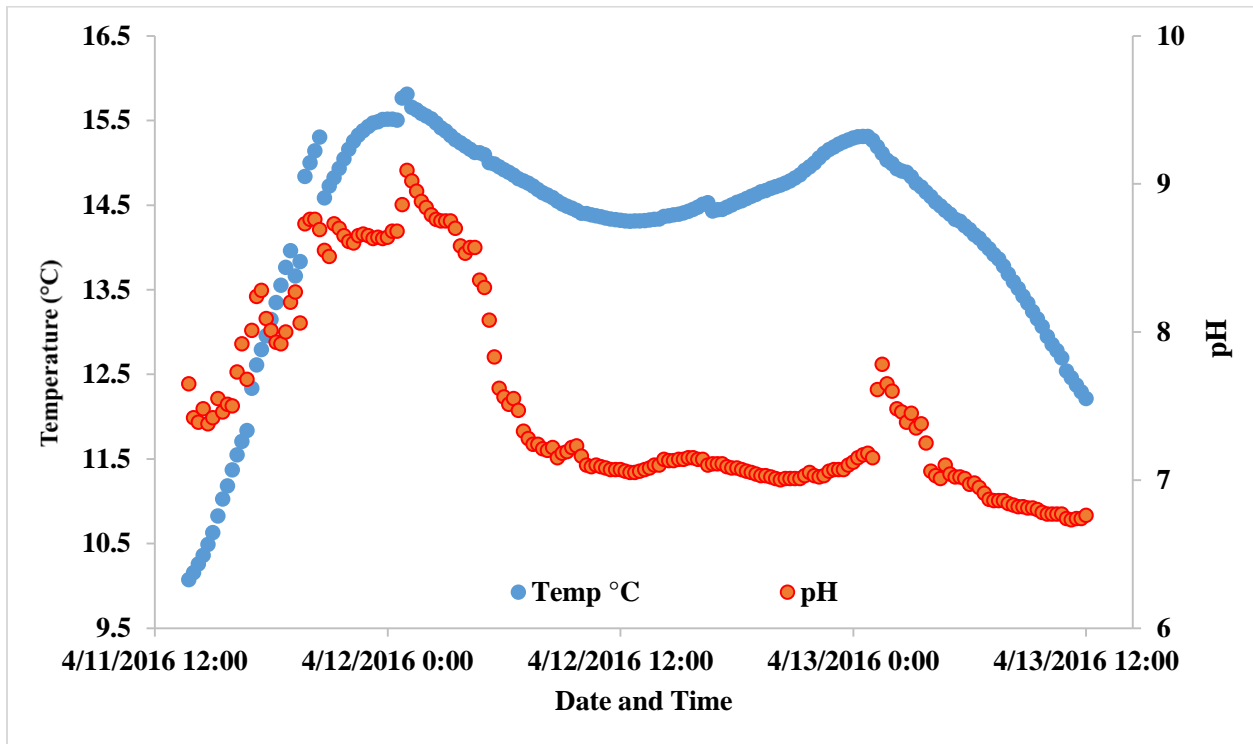


Figure S14. Temperature and pH data for *in situ* dissolution experiments.



## ADDITIONAL REFERENCES

1. Wang, Z.; Von Dem Bussche, A.; Kabadi, P. K.; Kane, A. B.; Hurt, R. H., Biological and environmental transformations of copper-based nanomaterials. *ACS Nano* **2013**, *7*, 8715-8727.
2. Adeleye, A. S.; Conway, J. R.; Perez, T.; Rutten, P.; Keller, A. A., Influence of extracellular polymeric substances on the long-term fate, dissolution, and speciation of copper-based nanoparticles. *Environ. Sci. Technol.* **2014**, *48*, 12561-12568.
3. Conway, J. R.; Adeleye, A. S.; Gardea-Torresdey, J.; Keller, A. A., Aggregation, Dissolution, and Transformation of Copper Nanoparticles in Natural Waters. *Environ. Sci. Technol.* **2015**, *49*, 2749-2756.
4. Wang, L.-F.; Habibul, N.; He, D.-Q.; Li, W.-W.; Zhang, X.; Jiang, H.; Yu, H.-Q., Copper release from copper nanoparticles in the presence of natural organic matter. *Water Res.* **2015**, *68*, 12-23.
5. Ma, R.; Stegemeier, J.; Levard, C.; Dale, J. G.; Noack, C. W.; Yang, T.; Brown, G. E.; Lowry, G. V., Sulfidation of copper oxide nanoparticles and properties of resulting copper sulfide. *Environ. Sci.: Nano* **2014**, *1*, 347-357.
6. Misra, S. K.; Dybowska, A.; Berhanu, D.; Croteau, M. N. I.; Luoma, S. N.; Boccaccini, A. R.; Valsami-Jones, E., Isotopically modified nanoparticles for enhanced detection in bioaccumulation studies. *Environ. Sci. Technol.* **2011**, *46*, 1216-1222.
7. Son, J.; Vavra, J.; Forbes, V. E., Effects of water quality parameters on agglomeration and dissolution of copper oxide nanoparticles (CuO-NPs) using a central composite circumscribed design. *Sci. Total Environ.* **2015**, *521*, 183-190.
8. Lowry, G. V.; Espinasse, B. P.; Badireddy, A. R.; Richardson, C. J.; Reinsch, B. C.; Bryant, L. D.; Bone, A. J.; Deonarine, A.; Chae, S.; Therezien, M., Long-term transformation and fate of manufactured Ag nanoparticles in a simulated large scale freshwater emergent wetland. *Environ. Sci. Technol.* **2012**, *46*, 7027-7036.
9. Gustafsson, J., Visual MINTEQ ver. 3.1. *KTH Department of Land and Water Resources Engineering, Stockholm, Sweden. Based on de Allison JD, Brown DS, Novo-Gradac KJ, MINTEQA2 ver 2011*, *4*, 1991.
10. Tegenaw, A.; Tolaymat, T.; Al-Abed, S.; El Badawy, A.; Luxton, T.; Sorial, G.; Genaidy, A., Characterization and Potential Environmental Implications of Select Cu-Based Fungicides and Bactericides Employed in US Markets. *Environ. Sci. Technol.* **2015**, *49*, 1294-1302.
11. Levard, C.; Mitra, S.; Yang, T.; Jew, A. D.; Badireddy, A. R.; Lowry, G. V.; Brown Jr, G. E., Effect of chloride on the dissolution rate of silver nanoparticles and toxicity to *E. coli*. *Environ. Sci. Technol.* **2013**, *47*, 5738-5745.